

Effects of Dynamical Quarks in UKQCD Simulations

Chris Allton

UKQCD Collaboration

Department of Physics, University of Wales Swansea, Singleton Park, Swansea SA2 8PP, United Kingdom

Recent results from the UKQCD Collaboration's dynamical simulations are presented. The main feature of these ensembles is that they have a fixed lattice spacing and volume, but varying sea quark mass from infinite (corresponding to the quenched simulation) down to roughly that of the strange quark mass. The main aim of this work is to uncover dynamical quark effects from these “matched” ensembles. We obtain some evidence of dynamical quark effects in the static quark potential with less effects in the hadronic spectrum.

1. Introduction

The UKQCD Collaboration has embarked upon a study of unquenching effects in QCD lattice simulations particularly in the static quark potential, light hadron spectrum and topological sector. The philosophy that UKQCD uses in this study is to simulate at a variety of sea quark masses, m^{sea} , but with a fixed the lattice spacing, a . This is in order to maintain, as far as possible, constant lattice systematic effects due to the finite-ness of a and the volume.

It is well known that the lattice cut-off, a , is a function of *both* the gauge coupling, β , and the dynamical quark mass, m^{sea} (see e.g. [1]). For this reason, the philosophy we have chosen is to simulate at points in the (β, m^{sea}) plane which have constant a . We term this the “matched” trajectory. The hope is that this procedure will disentangle lattice systematic effects (due to the finite-ness of a and volume) with unquenching effects. Any variation of a physical quantity along this matched trajectory can be attributed to unquenching effects rather than, e.g. $\mathcal{O}(a^2)$ effects.

This paper presents an overview of this work. See [2] for a full description.

2. Simulation Details

The standard Wilson gauge action was used together with the Clover $\mathcal{O}(a)$ -improved fermion action. The coefficient, c_{SW} , used in the Clover

term was non-perturbatively determined by the Alpha Collaboration [3].

A range of $(\beta, \kappa^{\text{sea}})$ values were chosen in order to maintain a constant value of the lattice spacing. This used the technology of [4]. The parameter values for the simulations are displayed in Table 1. The lattice volume used was $16^3 \times 32$ throughout.

Table 1 lists also the lattice spacing obtained from the Sommer scale, r_0 [5]. The first error listed is statistical, and the second (shown as $\frac{+x}{-y}$) is the systematic error from variations in the fit used for the static quark potential. The central values quoted were obtained using all potential data satisfying $\sqrt{2} \leq r \leq 8$. It can be seen that the last four simulations listed (i.e. those at $\kappa^{\text{sea}} = 0.1350, 0.1345, 0.1340$ and 0) are matched to within errors, with the $\kappa^{\text{sea}} = 0$ simulation corresponding to a quenched run.

The simulations at $\kappa^{\text{sea}} = 0.1355$ and 0.13565 were performed in order to study lighter sea quark masses and do not lie on the above matched trajectory.

Full details of autocorrelation times and other algorithmic issues can be found in [2].

3. The static potential

The static quark potential was determined for all our ensembles using the method originally proposed in [6] and using a variational basis of

Table 1

Lattice parameters together with measurements of a and quark masses.

β	κ^{sea}	c_{SW}	#conf.	a_{r_0} [Fm]	a_J [Fm]	$M_{PS}^{\text{unitary}}/M_V^{\text{unitary}}$
5.20	0.13565	2.0171	244	$0.0941(8)_{-0}^{+13}$	-	-
5.20	0.1355	2.0171	208	$0.0972(8)_{-0}^{+7}$	0.110_{-3}^{+4}	0.578_{-19}^{+13}
5.20	0.1350	2.0171	150	$0.1031(09)_{-1}^{+20}$	0.115_{-3}^{+3}	0.700_{-10}^{+12}
5.26	0.1345	1.9497	101	$0.1041(12)_{-10}^{+11}$	0.118_{-2}^{+2}	0.783_{-5}^{+5}
5.29	0.1340	1.9192	101	$0.1018(10)_{-7}^{+20}$	0.116_{-4}^{+3}	0.835_{-7}^{+7}
5.93	0	1.82	623	$0.1040(03)_{-0}^{+4}$	0.1186_{-15}^{+17}	1

“fuzzed” links [7].

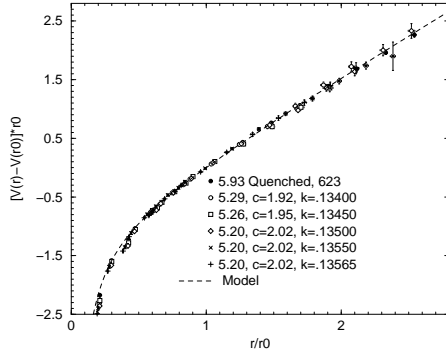


Figure 1. The static QCD potential expressed in units of r_0 . The dashed curve is a string model described in the text.

Figure 1 plots the static potential in units of r_0 . The zero of the potential has been set at $r = r_0$. The data are well described by the universal bosonic string model potential [8] which predicts

$$\begin{aligned}
 [V(r) - V(r_0)]r_0 &= (1.65 - e) \left(\frac{r}{r_0} - 1 \right) \\
 &- e \left(\frac{r_0}{r} - 1 \right). \quad (1)
 \end{aligned}$$

Of course, the fact that the scaled potential measurements all have the same value and slope at $r = r_0$ simply reflects the definition of r_0 . Figure 2 shows the deviations from this model potential for the matched ensembles. Here $e = \pi/12$ [8].

Overall there is no discernable difference between the ensembles at distance $r \approx r_0$. Furthermore, the data follow the string model very well. However, at shorter distances, $r < 0.5r_0$, there is a deviation from the string model, and a variation amongst the ensembles. This seems to be systematic in the sea quark mass – the deviation from the string model increases as m^{sea} decreases. In fact, careful correlated fits of the potential show that the parameter e in Eq.(1) increases by $18_{-10}^{+13}\%$ in going from the quenched to $\kappa^{\text{sea}} = .13500$ data. We note that the ensembles in Figure 2 are matched, and therefore we can exclude lattice systematics from the effects that we have observed. (Similar findings in the case of two flavours of Wilson fermions have been reported by the SESAM-T χ L collaboration [9] where an increase of $16 - 33\%$ was found.) Finally we note that there is no evidence of string breaking in our static quark potential. However the distance scales covered $r \lesssim 1.3fm$ is not large.

4. Hadronic Spectrum

In this section one of our main aims will be to uncover unquenching effects in the light hadron spectrum. Because we have a *matched* data set, any variation amongst our ensembles can be attributed to unquenching effects. However, the task of identifying variations is likely to be hard for those quantities which are primarily sensitive to physics at the same scale as that used to define the matching trajectory in the $(\beta, \kappa^{\text{sea}})$ parameter space (r_0 in this case). This is expected to be the case for the hadron spectrum considered here where the quark masses are still relatively heavy.

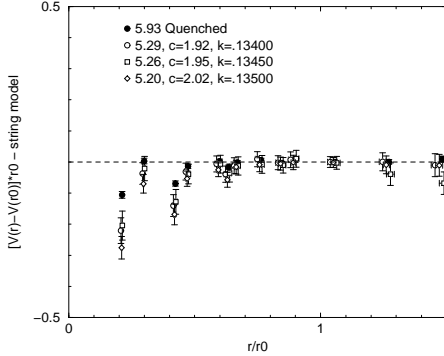


Figure 2. The difference between the static QCD potential expressed in physical units and the prediction of the string model described in the text. For clarity, only data from the matched ensembles are shown.

Two-point hadronic correlation functions were produced for each of the ensembles using interpolating operators for pseudoscalar, vector, nucleon and delta channels as described in [10]. Mesonic correlators were constructed using both degenerate and non-degenerate valence quarks, whereas only degenerate valence quarks were used for the baryonic correlators.

In the following, we review the main fitting procedures which were used to obtain the light hadron spectrum results. Further details of the fitting procedure can be found in [2].

We used the fuzzing procedures of [11] to generate correlators of the type LL, FL and FF where F denotes fuzzed, and L local operators.

Correlated fits were used throughout the fitting analysis of the correlation functions with the eigenvalue smoothing technique of [12] employed. A *factorising fit* was performed which combined the three fuzzed correlators LL, FL and FF together to extract a better estimate of the ground state parameters.

Full details of the fitting procedure can be found in [2].

4.1. The J parameter

In Figures 3 and 4 the vector meson masses and hyperfine splittings are plotted against the corresponding pseudoscalar masses for all the datasets. It is difficult to identify an unquenching signal from these plots - the data seem to overlay each other. Note that in [1], it was reported that there was a tendency for the vector mass to *increase* as the sea quark mass *decreases* (for fixed pseudoscalar mass). The observations for the present *matched* dataset imply that this may have been due to either an $\mathcal{O}(a)$ effect (since the dataset in [1] was not fully improved at this level) or a finite volume effect. The conclusion therefore is that it is important to run at a fixed a in order to disentangle unquenching effects from lattice artifacts or finite volume effects.

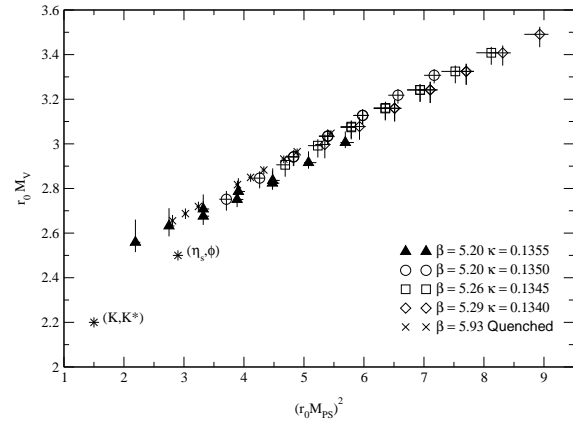


Figure 3. Vector mass plotted against pseudoscalar mass squared in units of r_0 , together with the experimental data points.

A possible explanation for the lack of convincing unquenching effects in our meson spectrum is the following. Our matched ensembles are defined to have a common r_0 value, so any physical quantity that is sensitive to this distance scale (and the static quark potential itself) will also, by definition, be matched. Our mesons, because they are composed of relatively heavy quarks, are examples of such quantities, and this is a possi-

ble reason why there is no significant evidence of unquenching effects in the meson spectrum.

A further point regarding hyperfine splitting in Figure 4 is that the lattice data for the *matched* ensembles tends to flatten as the sea quark mass decreases. (The quenched data has a distinctly negative slope, whereas the $\kappa^{\text{sea}} = 0.1350$ data is flat.) Thus the lattice data is tending towards the same behaviour as the experimental data which lies on a line with *positive* slope (independent of the value used for r_0). This behaviour is apparently spoiled by the unmatched run with $\kappa^{\text{sea}} = 0.1355$ (see Figure 4) which has a clear *negative* slope. However, the $\kappa^{\text{sea}} = 0.1355$ data does not satisfy the finite volume bound of [1], and therefore we can attribute the trend in this data to a lattice artefact.

We now study the J -parameter defined as [13]

$$J = M_V \left. \frac{dM_V}{dM_{PS}^2} \right|_{K, K^*}. \quad (2)$$

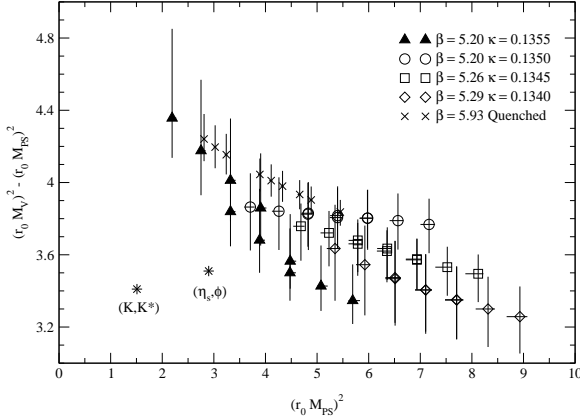


Figure 4. The hyperfine splitting.

In the context of dynamical fermion simulations, this parameter can be calculated in two ways. The first is to define a partially quenched J for each value of the sea quark mass. In this case, the derivative in (2) is with respect to variations in the valence quark mass (with the sea quark mass fixed). The second approach is to define J

along what we will term the ‘unitary’ trajectory, i.e. along $\kappa^{\text{sea}} = \kappa^{\text{val}}$. In Table 2, the results from both methods are given. These values of J are around 25% lower than the experimental value $J_{\text{expt}} = 0.48(2)$.

β	κ^{sea}	J
First Approach		
5.2000	0.1355	0.32_{-4}^{+2}
5.2000	0.1350	0.393_{-9}^{+10}
5.2600	0.1345	0.365_{-6}^{+6}
5.2900	0.1340	0.349_{-8}^{+7}
5.9300	0.0000	0.376_{-12}^{+9}
Second Approach		
-	-	0.35_{-2}^{+2}
Third Approach		
-	-	0.43_{-2}^{+2}

Table 2

J values from the various approaches as described in the text.

Finally we note that the physical value of J (i.e. that which most closely follows the procedure used to determine the experimental value of $J_{\text{expt}} = 0.48(2)$), should be obtained from extrapolating the results from the first approach to the physical sea quark masses. We call this the third approach. In order to perform this extrapolation, we extrapolate the three matched dynamical J values obtained from the first approach linearly in $(M_{PS}^{\text{unitary}})^2$ to $(M_{PS}^{\text{unitary}})^2 = 0$. M_{PS}^{unitary} is the pseudoscalar meson mass at the unitary point. The value for J from the third approach is presented in Table 2 and we note that it is approaching the experimental value for J .

The results from all three approaches are plotted in Figure 5, together with the experimental result. There is some promising evidence that the lattice estimate of J increases towards the experimental point as the sea quark mass decreases (see the J value from approaches 1 and 3).

Recently there has been a proposed ansatz for the functional form of M_V as a function of M_{PS}^2 [14]. Although this ansatz would be interesting to pursue, all our data have $M_{PS}/M_V \gtrsim 0.6$, and

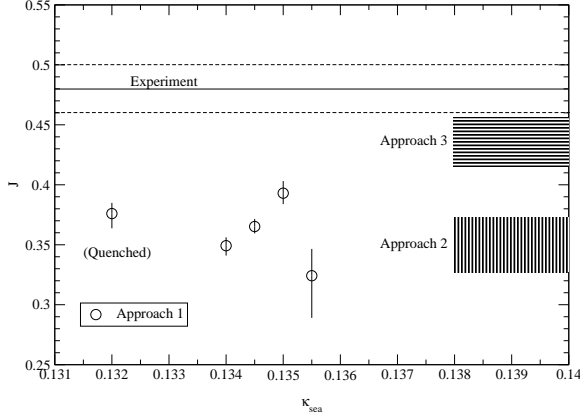


Figure 5. J versus κ^{sea} using the approaches as described in the text. Note that the quenched data points have been plotted at $\kappa^{sea} = 0.132$ for convenience. Approaches 2 & 3 are obtained after a chiral extrapolation and are shown as banded regions. The experimental value $J = 0.48(2)$ is also shown.

for this region, the ansatz of [14] is linear to high precision. Therefore we have chosen to interpolate our data with a simple linear function and await more chiral data before using the ansatz of [14].

4.2. Lattice spacing

This subsection presents a determination of a from the meson spectrum which complements that from r_0 .

A common method of determining a from the meson spectrum uses the ρ mass. However, this requires the chiral extrapolation of the vector meson mass down to (almost) the chiral limit which, as was discussed in the previous subsection, may be problematic. An alternative method of extracting the lattice spacing using the vector meson mass at the *simulated* data points (i.e. without any chiral extrapolation) was given in [15]. Using this method, we obtain the lattice spacing values as shown in Table 1 labelled a_J . Note that these are in general 10-15% larger than the values from Section 3 where the lattice spacing was determined from r_0 . A possible explanation for this discrepancy is that the potential and mesonic

spectrum are contaminated with different $\mathcal{O}(a^2)$ errors (or that the value $r_0 = 0.49$ fm is 10-15% too small!).

In order to investigate unquenching effects in the meson spectrum, we define the quantity

$$\delta_{i,j}(\beta, m^{sea}) = 1 - \frac{a_i(\beta, m^{sea})}{a_j(\beta, m^{sea})}, \quad (3)$$

where a_i is the lattice spacing determined from the physical quantity $i = \{M_\rho, M_K, f_\pi \dots\}$. Note that when $\delta_{i,j} = 0$, the lattice prediction of M_i with scale taken from M_j agrees with experiment. Thus δ is a good parameter to study unquenching effects. We expect that $\delta_{i,j}(\beta, m^{sea}) = \mathcal{O}(a^2)$ since we are working with a non-perturbatively improved clover action.

In Figure 6, $\delta_{i,j}$ is plotted against $(aM_{PS}^{unitary})^{-2}$ for the matched datasets. In this plot we have fixed $j = r_0$ and the various physical quantities i are $\sqrt{\sigma}$ (the string tension) and the hadronic mass pairs (M_{K^*}, M_K) & (M_ρ, M_π) . The method used to determine the scale a_i from these mass pairs is that of [15]. It is worth noting that the experimental point on this same plot would occur at an x -co-ordinate (depressingly) of $(aM_{D^*}^{unitary})^{-2} = (aM_\pi)^{-2} \approx 200$.

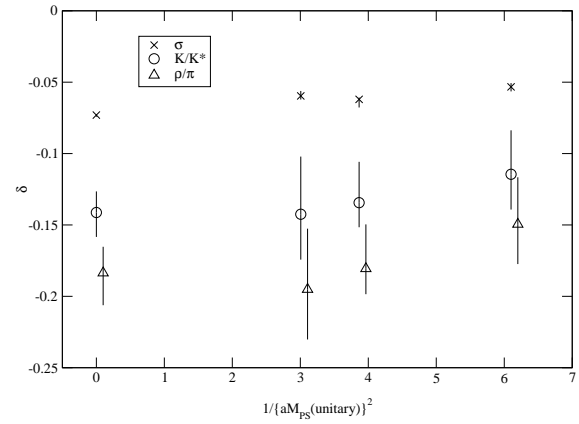


Figure 6. δ_i as a function of $1/(aM_{PS}^{unitary})^2$ for $i = \sqrt{\sigma}$ and the mass pairs (M_{K^*}, M_K) & (M_ρ, M_π) . δ_i is defined in eq.(3) with $j = r_0$.

Figure 6 does not show signs of unquenching

for quantities involving the hadronic spectrum i.e. the mass pairs (M_{K^*}, M_K) & (M_ρ, M_π) . However, there is evidence of unquenching effects when comparing the scale from r_0 with that from $\sqrt{\sigma}$ since the quenched value of $\delta\sqrt{\sigma}$ is distinct from the dynamical values.

One may wonder if the δ values may have been distorted by not choosing the simulation parameters (β, m^{sea}) exactly on the matched trajectory. In order to obtain a rough estimate of the effect of mis-matched value of β , we use the renormalisation group inspired ansatz for a_i [16,17]:

$$a_i(g_0^2) = \Lambda^{-1} f_{PT}(g_0^2) \times [1 + X_i f_{PT}(g_0^2)^{n_i}], \quad (4)$$

where $f_{PT}(g^2)$ is the usual asymptotic scaling function obtained from integrating the β -function of QCD and X_i is the coefficient of the $\mathcal{O}(a^n)$ lattice systematic. The functional form for $a(g_0^2)$ was originally applied for the quenched theory, but let us assume that it can also be applied in the unquenched case. Using Eq.(4), we see that a mismatch in β of $\Delta\beta$ would lead to a relative error in δ of

$$\frac{\delta(\beta + \Delta\beta) - \delta(\beta)}{\delta(\beta)} \approx -3\Delta\beta. \quad (5)$$

This shows that even an error in β of as much as $\Delta\beta \approx 0.01$ introduces a relative error in $\delta(\beta)$ of only 3%, ruling out the possibility that a significant distortion in δ could have occurred due to a mismatching in β .

4.3. Edinburgh Plot

In Table 1 the ratios M_{PS}/M_V are displayed for the unitary case $\kappa^{sea} = \kappa^{val}$. As can be seen the simulated data is a long way from the experimental value $M_\pi/M_\rho = 0.18$. Figure 7 shows the ‘Edinburgh plot’ (M_N/M_V v.s. M_{PS}/M_V) for all the data sets. There is no significant variation within the dynamical data as the sea quark mass is changed, but the dynamical data does tend to lie above the (matched) quenched data. This latter feature may be indicative of finite volume effects since these are expected to be larger in full QCD compared to the quenched case [18].

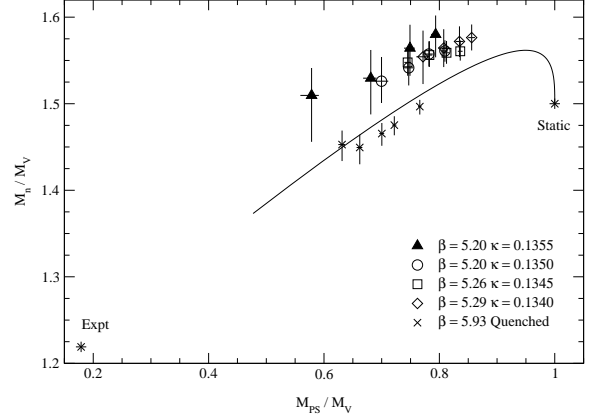


Figure 7. The Edinburgh plot for all the data sets. All degenerate κ^{val} correlators have been included. The phenomenological curve (from [19]) has been included as a guide to the eye.

5. Chiral Extrapolations

In [2] we used 3 approaches to perform the chiral extrapolations of hadron masses: ‘Pseudo-Quenched’; ‘Unitary Trajectory’; and a ‘Combined Chiral Fit’. In this publication we will refer only to the last approach. We take

$$\begin{aligned} \hat{M}(\kappa^{sea}; \kappa^{val}) &= A(\kappa^{sea}) + B(\kappa^{sea}) \hat{M}_{PS}(\kappa^{sea}; \kappa^{val})^2 \\ &= A_0 + A_1 \hat{M}_{PS}(\kappa^{sea}; \kappa^{sea})^{-2} \\ &+ [B_0 + B_1 \hat{M}_{PS}(\kappa^{sea}; \kappa^{sea})^{-2}] \hat{M}_{PS}(\kappa^{sea}; \kappa^{val})^2, \end{aligned}$$

using the nomenclature $\hat{M} \equiv aM$. The first argument of $\hat{M}(\kappa^{sea}; \kappa^{val})$ refers to the sea quark and the second to the valence quark.

The results of these extrapolations are shown in Table 3. We stress that this functional form for the extrapolation is not motivated by theory, but is used as a numerical analysis technique in order to test for evidence of unquenching effects. As can be seen from Table 3, the parameters A_1 and B_1 are compatible with zero (to 2σ) and therefore we conclude that there is no evidence of unquenching effects (i.e. there is no statistical variation in the fit parameters A and B with sea quark mass κ^{sea}).

hadron	A_0	A_1	B_0	B_1
Vector	$.492^{+10}_{-9}$	-0.004^{+2}_{-3}	0.61^{+4}_{-4}	$.015^{+9}_{-7}$
Nucleon	$.663^{+13}_{-15}$	0.006^{+3}_{-4}	1.23^{+6}_{-6}	$-.001^{+1}_{-1}$
Delta	$.84^{+2}_{-2}$	-0.002^{+5}_{-5}	0.91^{+8}_{-9}	$.02^{+2}_{-2}$

Table 3
Fit parameters from the Chiral Extrapolations

6. Conclusions

This paper attempts to uncover unquenching effects in the dynamical lattice QCD simulations at a fixed (matched) lattice spacing (and volume) and various dynamical quark masses. This approach allows a more controlled study of unquenching effects without the possible entanglement of lattice and unquenching systematics.

We see some sign of unquenching effects in the static quark potential at short distance, but no significant sign of unquenching effects in the meson spectrum. This is presumably since our dynamical quarks are relatively massive, and so the meson spectrum is dominated by the static quark potential. This potential is, by definition, matched amongst our ensembles at the hadronic length scale r_0 , and so any variation of the meson spectrum within our matched ensemble must surely be a “higher” order unquenching effect which is beyond our present statistics.

It is interesting to note that other work (using the same ensembles) has shown interesting unquenching effects in the glueball and topological sector [2].

7. Acknowledgements

The author wish to thank all of his collaborators in UKQCD. The support of the Particle Physics and Astronomy Research Council is gratefully acknowledged.

REFERENCES

1. UKQCD Collaboration, C.R.Allton *et al.*, Phys.Rev. **D60** (1999) 034507, [hep-lat/9808016](#).
2. UKQCD Collaboration, C.R.Allton *et al.*, [hep-lat/0107021](#).
3. ALPHA Collaboration, K. Jansen and R. Sommer, Nucl. Phys. **B530**, 185 (1998), [hep-lat/9803017](#).
4. UKQCD Collaboration, A. C. Irving *et al.*, Phys. Rev. **D58**, 114504 (1998), [hep-lat/9807015](#).
5. R. Sommer, Nucl. Phys. **B411**, 839 (1994), [hep-lat/9310022](#).
6. C. Michael, Nucl. Phys. **B259**, 58 (1985); S. Perantonis, A. Huntley, and C. Michael, Nucl. Phys. **B326**, 544 (1989).
7. APE Collaboration, M. Albanese *et al.*, Phys. Lett. **B192**, 163 (1987).
8. M. Luscher, Nucl. Phys. **B180**, 317 (1981).
9. SESAM Collaboration, G. S. Bali *et al.*, Phys. Rev. **D62**, 054503 (2000), [hep-lat/0003012](#).
10. UKQCD Collaboration, C. R. Allton *et al.*, Phys. Rev. **D49**, 474 (1994), [hep-lat/9309002](#).
11. UKQCD Collaboration, P. Lacock, A. McKerrell, C. Michael, I. M. Stopher, and P. W. Stephenson, Phys. Rev. **D51**, 6403 (1995), [hep-lat/9412079](#).
12. C. Michael and A. McKerrell, Phys. Rev. **D51**, 3745 (1995), [hep-lat/9412087](#).
13. UKQCD, P. Lacock and C. Michael, Phys. Rev. **D52**, 5213 (1995), [hep-lat/9506009](#).
14. D. B. Leinweber, A. W. Thomas, K. Tsushima, and S. V. Wright, [hep-lat/0104013](#).
15. C. R. Allton, V. Gimenez, L. Giusti, and F. Rapuano, Nucl. Phys. **B489**, 427 (1997), [hep-lat/9611021](#).
16. C. R. Allton, [hep-lat/9610016](#).
17. C. R. Allton, Nucl. Phys. Proc. Suppl. **53**, 867 (1997), [hep-lat/9610014](#).
18. A. Ukawa, Nucl. Phys. Proc. Suppl. **30**, 3 (1993).
19. S. Ono, Phys. Rev. **D17**, 888 (1978).